

Cyclic polypropylene pipeline coating interface strength with granular materials at low stress

Résistance cyclique d'interface de revêtement d'oléoduc en polypropylène avec des matériaux granulaires à faible contrainte

L. W. de Leeuw

University of Bristol, Bristol, United Kingdom

A. Diambra, M.S. Dietz, G. Mylonakis

University of Bristol, Bristol, United Kingdom

H. Milewski

TechnipFMC, Westhill, Aberdeenshire, United Kingdom

ABSTRACT: Laying subsea pipelines on dynamic seabeds comprising non-cohesive soils remains a challenge to geotechnical and pipeline engineers. Smooth polymer coatings are applied to protect the steel pipeline, but these relatively soft surfaces are subject to abrasion when pipes experience buckling or walking. Repeated start-up and shutdown cycles leads to cyclic movement across seabeds and even excess pore water pressure generation, so the interface strength may evolve in the process. This research subjects polypropylene pipeline coating specimens to submerged cyclic interface shear tests using two granular soils. Strength is observed to reduce by between ~10% and ~25% depending on the soil type and applied normal stress over the course of cycling to a cumulative horizontal displacement of ~1200mm. The reduction in strength is thought to occur in part due to grains creating striations and then repeatedly sliding up and down the same striation creating a smoothing effect for individual grains. Post-cyclic monotonic interface tests on the same surface specimen show an enhanced interface strength relative to the initial cyclic strength. This has implications for pipelines which may cycle locally and then walk or buckle to another location onto fresh un-sheared seabed sediments. Findings from this research are expected to reduce epistemic uncertainty in design and improve value for money in offshore engineering projects.

RÉSUMÉ: Cette recherche étudie le comportement des échantillons de pipeline revêtu en polypropylène partiellement enterré soumis à des essais cyclique de cisaillement de l'interface en utilisant deux sols granulaires. On observe que la résistance diminue entre ~ 10% et ~ 25% en fonction du type de sol et de la contrainte normale appliquée au cours du chargement cyclique, tandis que le déplacement horizontal cumulatif atteint ~1200 mm. La réduction de la résistance semble être due en partie au fait que les grains créent des stries sur l'interface, puis glissent à plusieurs reprises d'en bout à l'autre dans la même strie, créant ainsi un effet de lissage pour les grains individuels. Les essais d'interface monotoniques post-cycliques sur le même échantillon montrent une résistance d'interface améliorée par rapport à la résistance cyclique initiale. Cela a des implications pour les pipelines qui peuvent être d'abord soumis aux chargement cycles sur place, puis délogé vers un autre emplacement sur des sédiments de fonds marins non cisailés. Les résultats de cette recherche devraient réduire l'incertitude épistémique dans la conception des pipeliens et améliorer le rapport qualité-prix des projets d'ingénierie marine.

Keywords: interface; cyclic; polypropylene; sands; pipelines

1 INTRODUCTION

Offshore pipelines are often laid directly on the seabed. On clays this typically leads to pipe embedment, but on dynamic seabeds typically comprising loose sands, embedment may be transient or even absent. Pipelines are typically given a smooth polymer coating like polyethylene or polypropylene to provide protection from corrosion and impact damage, and to thermally insulate the hydrocarbon inside. Gaining a comprehensive, well constrained, understanding of the interface strength and correct quantification of the friction factor is essential to efficient and effective design.

The relationship between surface hardness of polymers and interface strength is well established (Saxena and Wong, 1984; Negussey *et al.*, 1989; O'Rourke *et al.*, 1990). In addition to the surface hardness the surface roughness normalised by D_{50} , referred to as effective roughness, also plays a role in influencing the interface friction coefficient (de Leeuw *et al.* 2019). Surface roughness evolves during shearing due to abrasion from grains creating striations, so it is expected that prolonged shearing increases the surface roughness and leads to an increase in strength.

As laid on dynamic seabeds, the smooth polymer-soil interface has a certain strength governed by the hardness and initial effective roughness of the surface. Thermally-induced axial loading in the pipeline can cause phenomena such as pipe walking or lateral buckling. During lateral buckling a feed-in zone develops where there is axial movement so striations may form in multiple orientations. During pipe movement, abrasion of the surface is expected to cause roughening through repeated cycles of buckling or walking leading to increased interface strength.

The present research investigates polypropylene pipeline coating interface strength using an interface shearbox in cyclic configuration up to approximately 1200mm of cumulative horizontal displacement. To replicate typical seabed pipe

conditions normal stress levels between approximately 2.5kPa and 35kPa were selected (O'Rourke, *et al.* 1990; White and Cathie, 2011) and two test sands used with D_{50} of 0.88mm and 0.35mm. A shearing rate of approximately 0.75mm/minute was applied.

2 MATERIALS

2.1 Granular materials

Two granular soils, known well in the literature, were used for this testing; Hostun Sand D_{50} 0.35mm and Leighton Buzzard 14-25 D_{50} 0.88mm. Their particle size distributions are shown in Figure 1. In this work, particle angularity has not been considered and is the subject of future research.

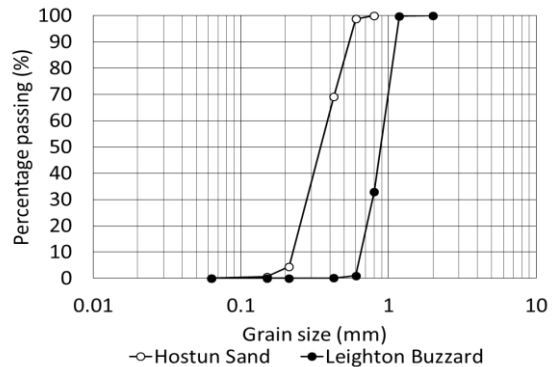


Figure 1. Particle size distribution of test sands

2.2 Polypropylene surfaces

Two specimens of polypropylene coating were used for this testing which were obtained by removal from already manufactured steel pipe. Heat was applied to soften the adhesive and the coating could then be peeled from the pipe. The samples were then flattened at 160°C under 20kg masses and cooled to ambient laboratory temperature still under load. Specimens, also referred to as counterfaces, were selected for testing which had as uniform a surface as possible with no obvious blemishes, seams, or manufacturing artefacts within the shearing area. Specimen selection in this way was to reduce uncertainty

between test specimens but is not reflective of real-world conditions where all such artefacts and more will be present.

3 METHODOLOGY

3.1 Testing apparatus

Interface testing was carried out using the Winged Direct Shear Apparatus (Lings and Dietz, 2004) developed at University of Bristol, to accurately measure shear forces at low stress. A pair of wings is attached to the sides of the upper frame, through which the load is applied via ball races. The point of application of the load is close to the centre of the shearbox and dilation can take place unimpeded. Support blocks and linear bearings ensure freedom of longitudinal movement whilst maintaining the loading arms in the horizontal plane irrespective of top cap vertical displacement or rotation. This arrangement allows better articulation of the force transmission system so that volumetric changes are not impeded and normal stress estimates are reliable.

Polypropylene surfaces were secured to an aluminium load pad with a series of perimeteral countersunk bolts to give a flat surface. During sample preparation a gap is created between shearbox halves to ensure shearing between soil and surface and not between the lower frame and the interface top cap of the shearbox. The gap size was 4mm in both cases to ensure sufficient room for settlement without shearbox halves coming into contact. Thin flexible rubber strips were used around the edges to prevent sample loss during testing.

The shearbox was instrumented with four Linear Variable Differential Transformers (LVDTs); three to measure vertical displacement at the centre, the leading edge, and the trailing end of the top cap, and one to measure horizontal displacement. An S-type 500N load cell was used to measure the force required to restrain the upper half during shearing measuring in tension or compression depending on the cycle direction.

3.2 Sample fabrication

Samples were prepared upside down in a sand-over-surface configuration before inverting to test in a surface-over-sand configuration (Figure 2). With the appropriate gap between surface and lower frame preinstalled using grub screws which are later retracted through the load pad, the soil was slowly poured into the shearbox through a funnel ensuring zero drop height (Figure 2a) to create a mound of loosest possible density as described in Miura *et al.* (1997). The mound was then gently spread to create a flat-topped sample on top of which an aluminium block is then placed and vibrated to encourage sample compaction to the desired relative density (Figure 2b). When densified, the upper half is removed and excess soil cleared and an aluminum plate is secured across the top of the sample (Figure 2c). The sample is inverted in one smooth movement to ensure minimal sample disturbance (Figure 2d) and is then ready for positioning in the shear carriage. Sample saturation is carried out by gently flooding the shear carriage prior to the load being applied and consolidation occurring.

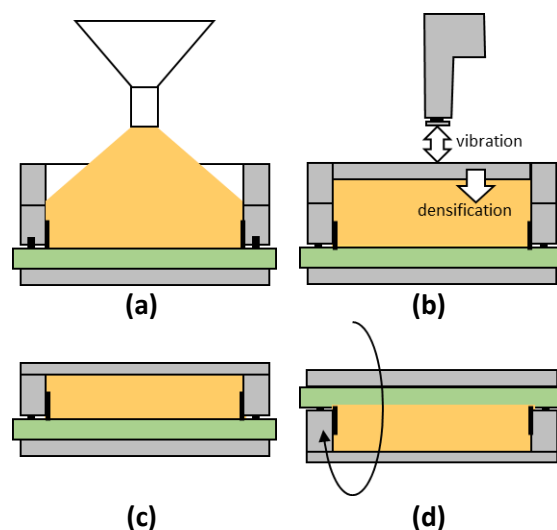


Figure 2. Schematic drawing of sample deposition into the inverted interface shearbox (a), vibration and densification (b), securing of the box floor (c), and the interface shearbox as arranged in its test configuration (d).

3.3 Test procedure

Cyclic interface shear tests were carried out on both test sands in a dense condition of approximately 70% relative density, at normal stresses of 2.5kPa, 10kPa, and 35kPa. Although seabed conditions are typically loose, and density does have a modest effect on interface shear stress, dense tests were considered more practical due to the large settlements that occur during cyclic shearing of loose soils.

Starting from a neutral position, shearing was cycled approximately 50 times with approximately 12mm travel for each half cycle individual pass corresponding to approximately 1200mm cumulative horizontal displacement. Due to the nature of the testing apparatus, shearing was non-continuous with short pauses of a few seconds between automatically-triggered reversals. The shear rate was approximately 0.75mm/minute and tests were carried out submerged with the water at ambient laboratory temperatures of approximately 21°C.

After cyclic testing was complete, monotonic tests were carried out on the same surfaces using freshly prepared sand samples to replicate the conditions of a pipe that has traversed the seabed and come into contact with fresh, unsheared soil.

4 TESTING PROGRAMME

The normal stress, relative density as fabricated, and void ratio as fabricated for each test are detailed in Tables 1, 2, and 3. Included also is the post-consolidation relative density and void ratio which was determined after sample saturation and once the normal load had been applied and consolidation was complete. The figures for relative density and void ratio post consolidation represent the soil condition at the commencement of shearing. Table 1 details the initial monotonic interface tests, Table 2 details the cyclic tests, and Table 3 details the post-cyclic reloaded tests on freshly prepared sand samples.

Table 1. Summary of test sample parameters as fabricated and post initial consolidation for monotonic interface shear tests.

Test ID	σ'_v (kPa)	Dr_{fab}	Dr_{con}	e_{fab}	e_{con}
HS02_I	2.09	0.70	0.71	0.73	0.73
HS05_I	5.16	0.70	0.71	0.73	0.73
HS10_I	11.30	0.70	0.75	0.73	0.71
HS20_I	21.52	0.70	0.76	0.74	0.71
HS35_I	36.86	0.70	0.84	0.73	0.68
LB02_I	2.02	0.77	0.81	0.60	0.59
LB05_I	5.09	0.78	0.84	0.60	0.58
LB10_I	11.23	0.79	0.82	0.60	0.59
LB20_I	21.45	0.76	0.84	0.61	0.58
LB35_I	36.79	0.73	0.88	0.61	0.57

Table 2. Summary of test sample parameters as fabricated and post initial consolidation for cyclic interface shear tests.

Test ID	σ'_v (kPa)	Dr_{fab}	Dr_{con}	e_{fab}	e_{con}
HS02_IMR	2.09	0.70	0.72	0.73	0.73
HS10_IMR	11.30	0.70	0.76	0.73	0.71
HS35_IMR	36.86	0.70	0.75	0.73	0.71
LB02_IMR	2.04	0.70	0.71	0.62	0.62
LB10_IMR	11.24	0.70	0.76	0.62	0.60
LB35_IMR	36.80	0.70	0.78	0.62	0.60

Table 3. Summary of test sample parameters as fabricated and post initial consolidation for monotonic post-cyclic reloading tests on fresh sand samples.

Test ID	σ'_v (kPa)	Dr_{fab}	Dr_{con}	e_{fab}	e_{con}
HS02_IpMR	2.09	0.70	0.72	0.73	0.73
HS05_IpMR	5.15	0.70	0.73	0.73	0.72
HS10_IpMR	11.29	0.70	0.75	0.73	0.72
HS20_IpMR	21.52	0.70	0.76	0.73	0.71
HS35_IpMR	36.85	0.70	0.79	0.73	0.70
LB02_IpMR	2.05	0.70	0.70	0.62	0.62
LB05_IpMR	5.05	0.70	0.73	0.62	0.62
LB10_IpMR	11.05	0.70	0.72	0.62	0.62
LB20_IpMR	21.05	0.70	0.73	0.62	0.62
LB35_IpMR	36.05	0.70	0.78	0.62	0.60

5 RESULTS: MONOTONIC TESTS

Figure 3 presents the shear stress-horizontal displacement for initial monotonic interface tests conducted on the two test sands. In both cases, and at all five stress levels, shear stress rapidly increases to a maximum value before plateauing and becoming largely stable for the remainder.

Strength envelopes for the interface strength are presented in Figure 4 including the interface angle of friction, δ , in the caption. The ratio between ultimate shear stress (determined as the average shear stress between 10 and 12mm horizontal displacement) and normal stress, referred to as strength, compared to normal stress is presented in Figure 5 and shows that for both test sands there is a significant enhancement in strength at very low stress.

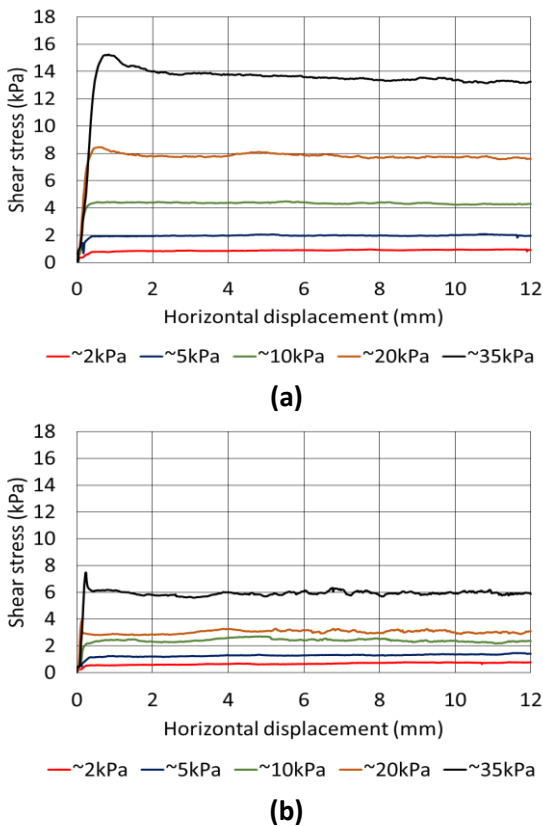


Figure 3. Monotonic shear stress-displacement curves for Hostun Sand (a) and Leighton Buzzard 14-25 sand (b) showing rapid initial increase in strength which is then largely stable for the duration.

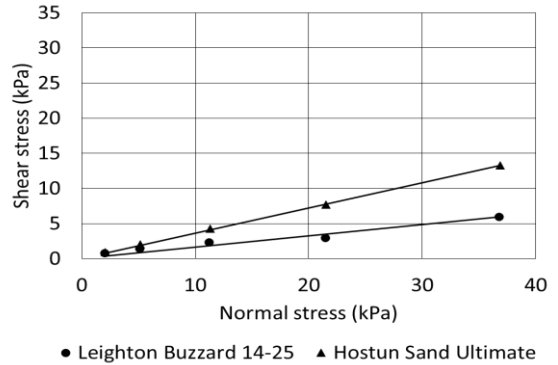


Figure 4. Interface shear strength envelopes for Hostun Sand $\delta = 20^\circ$ (a) and Leighton Buzzard 14-25 $\delta = 9^\circ$ (b).

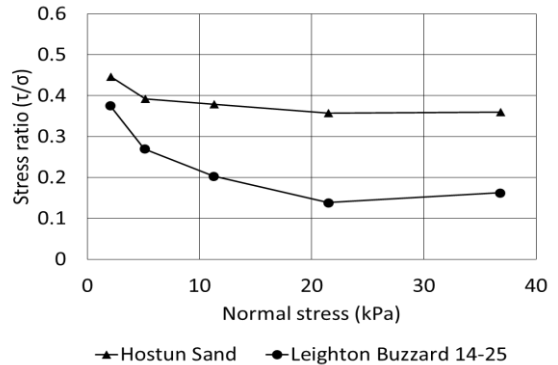


Figure 5. Variation of interface stress ratio (τ/σ) with normal stress σ'_v for Hostun Sand and Leighton Buzzard 14-25.

Figure 5 shows that between $\sigma'_v \sim 35\text{kPa}$ and $\sigma'_v \sim 2\text{kPa}$ the stress ratio changes by approximately 0.75 and 2.25 for Hostun Sand and Leighton Buzzard 14-25 respectively. For a given surface of the same roughness, a smaller particle experiences a greater effect due to the relative size of the particle to the topography of the surface. The term normalised roughness (Uesugi and Kishida, 1986) is adapted by Jardine *et al.* (1993) and used to normalise the roughness by D_{50} with the expression $R_{norm} = R_a/D_{50}$ where R_a is the average roughness defined as the average value of maximum deviations from the centre line. Roughness of the surfaces was measured using an Alicona InfiniteFocus non-contact profilometer and yielded R_a values of 0.849 and 0.724 microns for

the Hostun Sand counterface and Leighton Buzzard 14-25 counterface respectively. Normalised roughness for the Hostun Sand interface is 0.00243 and for Leighton Buzzard 14-25 sand interface is 0.00082. The effective roughness of the surface for Hostun Sand was nearly three times greater than for Leighton Buzzard 14-25 which offers some explanation for the difference in interface strength observed between these two test sands.

6 RESULTS: CYCLIC TESTS

Figure 6 shows typical results for shear stress-horizontal displacement for cyclic interface shear tests. Shear stress rapidly increases to a maximum and then remains largely stable

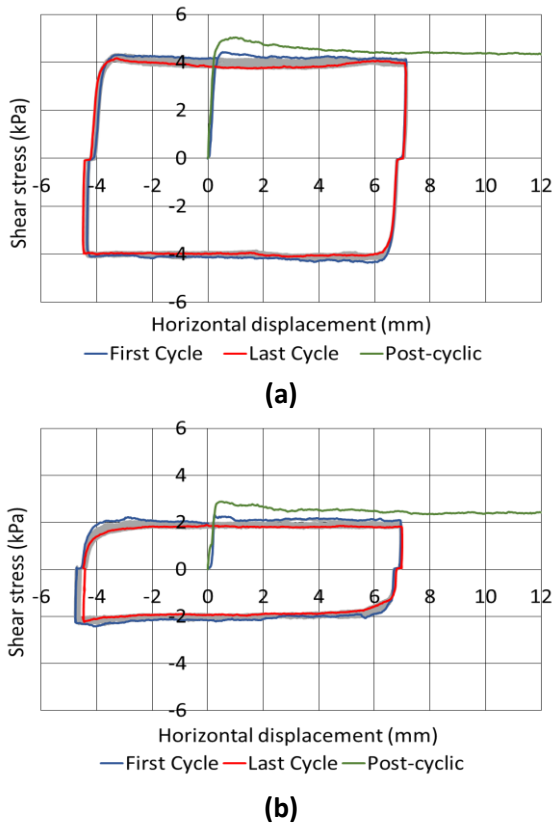


Figure 6. Cyclic shear stress-displacement curves at $\sigma'_v \sim 10\text{kPa}$ for Hostun Sand (a) and Leighton Buzzard 14-25 (b) with later reloaded test data superimposed in green.

Typical plots of vertical-horizontal displacement are shown in Figure 7. The rate of sample contraction during shearing reduces with each cycle. Settlement appears to be asymmetric between extremes of each pass which may be caused by large scale topography changes across the surfaces or the result of rotation of the top cap. Variations are in the order of 0.05mm over 12mm of travel so are considered negligible and symptomatic of experimental data using real industrial materials.

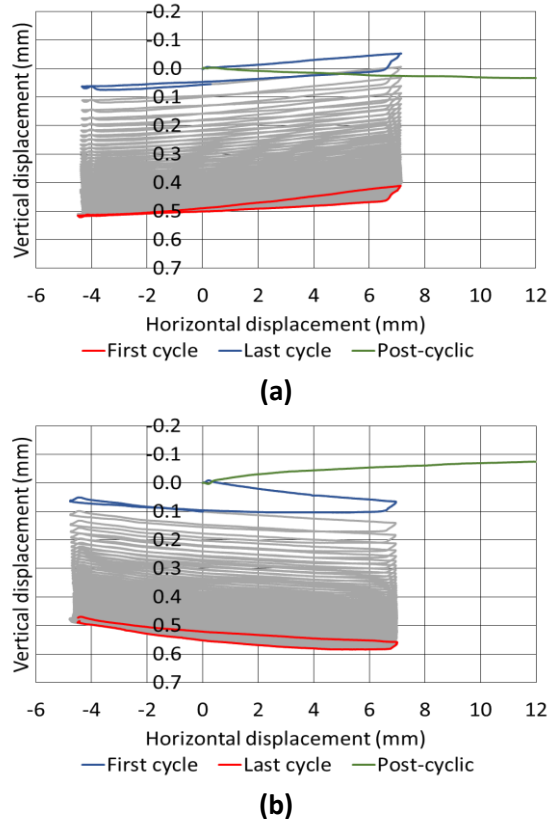


Figure 7. Cyclic vertical-horizontal displacement curves at $\sigma'_v \sim 10\text{kPa}$ for Hostun Sand (a) and Leighton Buzzard 14-25 (b) with later reloaded test data superimposed in green.

It is helpful to normalise the strength by the strength of the first cycle and these points are presented, with best fit curves, in Figure 8 for Hostun Sand and Figure 9 for Leighton Buzzard 14-25 sand. The data show an initial reduction in strength which gradually settles so that generally strength becomes quasi-constant.

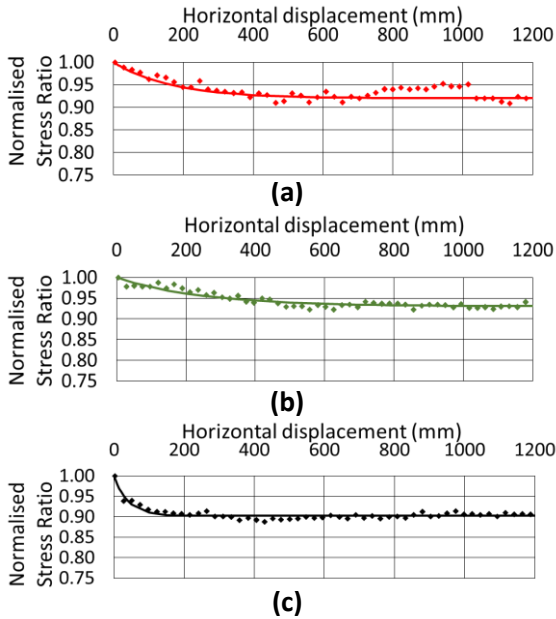


Figure 8. Cyclic normalised strength (τ/σ'_v) reduction with cumulative horizontal displacement for Hostun Sand at $\sigma'_v \sim 2.kPa$ (a), $\sim 10kPa$ (b), and $\sim 35kPa$ (c)

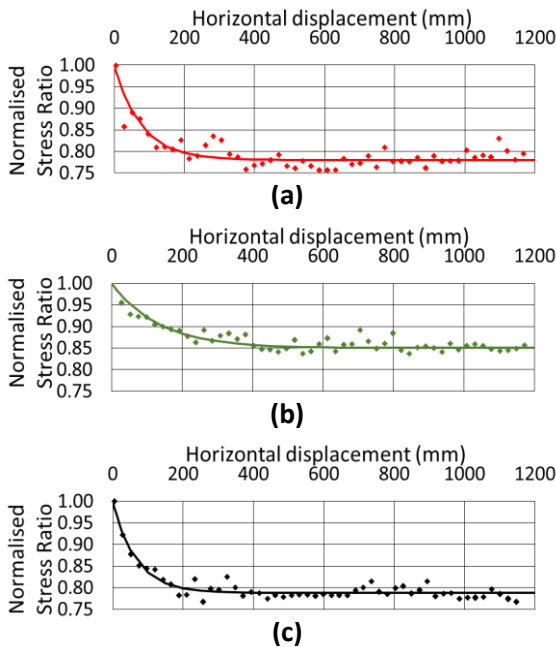


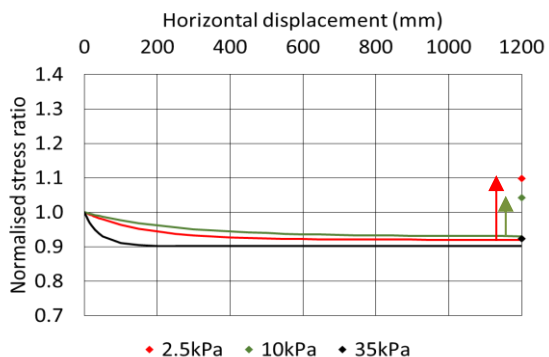
Figure 9. Cyclic normalised strength (τ/σ'_v) reduction with cumulative horizontal displacement for Leighton Buzzard 14-25 at $\sigma'_v \sim 2.5kPa$ (a), $\sim 10kPa$ (b), and $\sim 35kPa$ (c)

Generally, interface strength with Hostun Sand experienced a strength reduction of $\sim 10\%$ and Leighton Buzzard 14-25 of between $\sim 15\%$ and $\sim 20\%$. There is some variation with stress level but there is no discernible trend in these data and natural variability between polypropylene counterfaces cannot be accounted for and may be responsible.

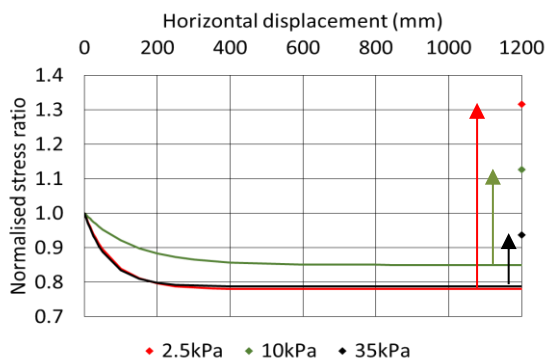
7 RESULTS: POST-CYCLIC RELOADING

Monotonic interface tests were carried out after cyclic testing on the same surfaces using freshly prepared sand samples to compare the interface strength after 1200mm of cycling. Stress-displacement and vertical against horizontal displacement for the reloaded tests are included, marked in green, in Figures 6 and 7. The results are normalised against the strength of the first cycle strength and plotted as points in Figure 10 for each stress level. Best fit lines from Figures 8 and 9 are also included.

At $\sim 2.5kPa$ and $\sim 10kPa$ the interface strength has increased relative to the first cycle for both test sands. At $\sim 35kPa$ the strength has increased relative to the final strength during cyclic but is slightly reduced compared to the first cycle strength. Although Leighton Buzzard 14-25 interfaces experienced the greatest reduction in strength through cycling, they also give the largest strength improvement relative to their initial strength (up to a $\sim 30\%$ and $\sim 12\%$ improvement at $\sim 2.5kPa$ and $\sim 10kPa$ respectively). This compared to Hostun Sand where the post cyclic interface strength showed a more modest $\sim 10\%$ and $\sim 4\%$ increase for $\sim 2.5kPa$ and $\sim 10kPa$ respectively. For both Hostun Sand and Leighton Buzzard 14-25 post-cyclic interface strength at $\sim 35kPa$ was approximately 6% lower but still higher than the final cyclic strength.



(a)



(b)

Figure 10. Post-cyclic reloaded strength improvement normalised to the initial strength and cyclic test data for Hostun Sand (a) and Leighton Buzzard 14-25 sand (b).

8 CONCLUSIONS

After relatively modest cumulative horizontal displacements the initial trend for reducing interface shear strength abates and a constant resistance is mobilised. Similarly, vertical displacement follows a similar trend where settlement per cycle reduces over the period of the test. Resetting the experiment with the same surface already cyclic-tested but on a freshly prepared sand sample resulted in a significant increase in strength relative to the strength of the first cycle.

Such behaviour requires further work to fully understand but could have important design

implications where subsea pipes may displace and become striated and then come to lie on undisturbed soils.

9 ACKNOWLEDGEMENTS

The authors wish to acknowledge and thank TechnipFMC for their generous support and provision of test materials which enabled this research to be carried out.

10 REFERENCES

- de Leeuw, L.W., Diambra, A., Dietz, M.S., Mylonakis, G., Milewski, H. 2019. In: *7th International Symposium on Deformation Characteristics of Geomaterials*, Glasgow, UK.
- Jardine, R.J., Lehane, B.M., Everton, S.J. 1993. Friction coefficients for piles in sands and silts, In: *Offshore Site Investigation and Foundation Behaviour*, Society for Underwater Technology, London, UK, **28** (1), 25-37.
- Lings, M.L. Dietz, M.S. 2004. An improved direct shear apparatus for sand, *Geotechnique* **54** (4), 245-256.
- Miura, K., Maeda, K., Toki, S. 1997. Method of measurement for the angle of repose of sands, *Soils and Foundations* **37** (2), 89-96.
- Negussey, D. Wijewickreme, W.K.D., Vaid, Y.P. 1989. Geomembrane interface friction, *Canadian Geotechnical Journal* **26** (1), 165-169.
- O'Rourke, T.D., Druschel, S.J., Netravali, A.N. 1990. Shear strength characteristics of sand-polymer interfaces, *Journal of Geotechnical Engineering* **116** (3), 451-469.
- Saxena, S.K. Wong, Y.T. 1984. Friction characteristics of a geomembrane. In: *Proceedings of the International Conference on Geomembranes*, Denver, 187-190.
- Uesugi, M. Kishida, H. 1986. Frictional resistance at yield between dry sand and mild steel. *Soils and Foundations* **24** (4), 139-149.
- White, D.J. Cathie, D.N. 2011. Geotechnics for subsea pipelines. In: *Proceedings of the 2nd International Symposium on Frontiers in Offshore Geotechnics*, Perth, Australia, pp. 87-123.